"Repeatability of Regional Pulmonary Functional Metrics of Hyperpolarized 129Xe Dissolved Phase MRI"

Andrew D. Hahn, PhD[1], Jeff Kammerman, MS[1], Michael Evans, MS[2], Wei Zha, PhD[1], Robert V. Cadman, PhD[1], Keith Meyer, MD[3], Nathan Sandbo, MD[3], Sean B. Fain, PhD[1,4,5]

[1]Department of Medical Physics, University of Wisconsin, Madison, WI

[2]Department of Biostatistics and Medical Informatics, University of Wisconsin, Madison, WI

[3]Department of Medicine, University of Wisconsin, Madison, WI

[4]Department of Radiology, University of Wisconsin, Madison, WI

[5]Department of Biomedical Engineering, University of Wisconsin, Madison, WI

Abstract

Background: MRI of hyperpolarized ^{129}Xenon (HP ^{129}Xe) is increasingly utilized for investigating pulmonary function. Solubility of HP ^{129}Xe in lung tissue, blood plasma (Barrier), and red blood cells (RBC), with unique chemical shifts, enables spectroscopic imaging of potential imaging biomarkers of gas exchange and microstructural pulmonary physiology.

Purpose: Quantifying global average and regional repeatability of Barrier:gas, RBC:gas and RBC:Barrier ratios derived from dissolved-phase ^{129}Xe imaging and their dependence on inter-visit changes in lung inflation volume.

Study Type: Prospective.

Population: 14 healthy volunteers. One subject was unable to complete the study resulting in 13 subjects for analysis (8 female, 5 male, ages 24–69, 53.8±13.9).

Field Strength: 1.5 Tesla.

Assessment: Subjects were imaged using a 3D radial 1-point Dixon method to separate Barrier and RBC component signals, at 2 different time points, with approximately 1 month between visits. RBC:Gas, Barrier:Gas and RBC:Barrier measures were compared across time and with pulmonary function tests (PFTs).

Statistical Tests: Repeatablilty was quantified using Bland Atlman plots, coefficient of repeatability, coefficient of variation (CV) and intra-class correlation coefficients (ICC). Dependence of imaging measures on PFTs and lung volume was evaluated using Spearman and Pearson correlation coefficients, respectively. Statistical significance was determined by F-test for intra-class correlations, and t-test for Spearman correlations and regression.

Corresponding author: Sean B. Fain, sfain@wisc.edu, phone: 608.263.0090, fax: 608.265.9840, **Institution of Origination** University of Wisconsin – Madison, Department of Medical Physics, 1111 Highland Ave., Room 1005, Madison, WI 53705-22.

Results: Mean RBC:Gas, Barrier:Gas and RBC:Barrier had CVs of 19.2%, 20.0% and 11.5%, respectively, and had significant ICCs, equal to 0.78, 0.79 and 0.92, respectively. Inter-visit differences in RBC:Barrier were significantly correlated with inter-visit differences in DLCO (r=0.93,P=0.007). Significant correlations with inter-visit lung volume differences and inter-visit differences in mean RBC:Gas (r=−0.73,P=0.005) and Barrier:Gas (r=−0.69,P=0.009) were found.

Data Conclusion: Three commonly used ^{129}Xe MRI based measures of gas-exchange show good repeatability, particularly Barrier:RBC ratio which did not depend on lung inflation volume and was strongly associated with inter-visit changes in DLCO.

Keywords

Xenon; MRI; Repeatability; Lung

INTRODUCTION

MRI of hyperpolarized ^{129}Xenon (HP ^{129}Xe) is an attractive and increasingly utilized technique for investigating pulmonary function [1]. Hyperpolarized ^{129}Xe has been demonstrated to provide similar quantitative measures of lung function as HP ^{3}He, especially for functional ventilation imaging [2]. HP ^{129}Xe gas is partially soluble in lung tissue and blood plasma (commonly referred to as the diffusion "barrier"), and red blood cells (RBC) [3]. Each of the barrier and RBC ^{129}Xe compartments experience unique chemical shifts, at 198 ppm and 217 ppm respectively, relative to the gas-phase portion of the signal [4] allowing all three to be measured separately using a variety of spectroscopy and spectroscopic imaging techniques [4–8]. Particular biomarkers of interest for dissolved phase spectroscopic imaging include Barrier:Gas, RBC:Gas and RBC:Barrier ratios that have been used to study whole lung and regional pathology of gas exchange in interstitial lung disease, specifically idiopathic pulmonary fibrosis (IPF) [9].

Measuring the repeatability of ^{129}Xe MRI based gas-exchange metrics is crucial for determining their utility and variability for quantitative characterization and monitoring of disease [10]. However, there are limited repeatability studies of Barrier:Gas, RBC:Gas and RBC:Barrier ratios derived from global lung spectroscopy, and especially spectroscopic imaging. Moreover, few studies to date have systematically assessed the dependence of the repeatability of these ratios on lung inflation volume. In a handful of prior studies repeatability has been reported for global lung HP ^{129}Xe MR spectroscopy measures of gas-exchange or microstructural tissue properties [11] including both septal thickness and alveolar surface-to-volume measurements with chemical shift saturation recovery (CSSR) [12] and repeatability of whole lung RBC:Barrier ratios [13,14]. The dependence of global HP ^{129}Xe MR spectroscopy measures on lung inflation volume has also been investigated for Barrier:Gas and RBC:Gas ratios [12–15] but not for spectroscopic imaging. A recent work has investigated the repeatability of regional CSSR-based measures, and compared these with ^{129}Xe dissolved phase 3D spectroscopic imaging measures [16], although dependence on lung inflation volume was not assessed. While these prior results indicate that controlling for lung volume is important, regional measures may have different sensitivity to variations in lung inflation that could be crucial for separating changes due to

ongoing disease processes from spurious variability in breath hold volumes and identifying image biomarkers for future clinical research studies.

The goal of this work, therefore, is to directly study the repeatability of global average and regional measures of Barrier:Gas, RBC:Gas, and RBC:Barrier ratios acquired with a 3D radial 1-point Dixon sequence utilized in multiple research studies of lung disease [8,9,13] in an older healthy subject cohort similar in age range to the typical onset of IPF [17].

MATERIALS AND METHODS

Study Design

A total of 14 healthy volunteers underwent HP ^{129}Xe MRI on a 1.5T scanner (General Electric, Waukesha, WI) using a quadrature vest coil tuned to the ^{129}Xe resonant frequency of 17.66 MHz @ 1.5T (Clinical MR Solutions, Brookfield, WI). One subject was unable to complete the imaging study due to concerns related to low oxygen saturation during imaging; this subject experienced consecutive post-dosing decreases in oxygen saturation of >10%, exceeding the 5% decrease considered to be significant per the study protocol, and was thus advised to not continue with the study. This resulted in 13 subjects for analysis (8 female, 5 male, ages 24–69 with mean 53.8 and standard deviation 13.9). The study was HIPAA compliant and informed consent was obtained in accordance with approved Institutional Review Board (UW IRB 2013–0266 and UW IRB 2014–1572) and investigational new drug (FDA IND# 118077) protocols. Subjects were required to be a current non-smoker with no history of lung disease, heart disease, or cancer. Each subject was imaged under identical protocols at 2 different time points, with approximately 1 month between visits (range 28–40 days, mean 31.7 days, standard deviation 4.3 days). Pulmonary function test (PFT) measurements of FEV1 and FVC by spirometry and DL_{CO} by the single-breath method were obtained immediately prior to imaging at both time points in 7 of the 13 subjects. Percent predicted (%p) values for PFT measures were calculated based on reference values of global lung function initiative (GLI)[18]. Study population demographics and PFTs are provided in Table 1.

^{129}Xe Preparation and Delivery

The ^{129}Xe gas (85% isotopically enriched; Linde Gases, Stewartsville NJ) was hyperpolarized via spin-exchange optical pumping [19] using a commercially available polarizer (model 9820, Polarean, Durham, NC). A total of 1 liter of HP ^{129}Xe gas was cryogenically accumulated and subsequently thawed into an Tedlar bag fitted with a quick-disconnect attachment. Polarization of the collected gas ranged from 13–27% at a polarization measurement station (model 12881, Polarean, Durham NC).

Subjects were administered the HP ^{129}Xe gas using a non-rebreather mask with a quick-disconnect attachment fitted to the input port. Subjects were coached to exhale to FRC, during which the bag of HP ^{129}Xe was connected to the mask input port. The subject was coached to inhale the entire 1-liter bag followed by a breath hold of approximately 15 seconds. Residual, un-inhaled, gas remaining in the bags was measured and recorded following each exam.

Image Acquisition

[129]Xe MRI was performed using a 3D radial pulse sequence capable of the interleaved acquisition of both gas- and dissolved-phase images during a single ~15 second breath hold [8]. Specific acquisition parameters were: FOV = 40 cm, matrix = 64×64×64, TR = 7.5 ms, BW = 31.25 kHz, flip-angles (dissolved/gas) = 22°/0.5°, 1001 radial projections. Following imaging of the first four subjects, a technical advancement in the pulse sequence was made allowing for removal of undesirable gas-phase signal contaminating the dissolved phase [20]. This was accomplished by acquisition using a similar multi-echo (2 echoes, TE = 3.3ms) sequence as described in [20]. Barrier and RBC component signals were separated using a 1-point Dixon method, and the appropriate TE was determined using a separate calibration scan, each as previously described [8].

Proton MRI of the chest was also acquired to facilitate generation of a segmented mask of the lungs for HP [129]Xe analysis and determination of actual lung volumes. Subjects inhaled a volume matched bag of room air (1-liter), administered in a manner identical to the HP [129]Xe gas, and performed a 13-second breath hold during which a 3D radial MRI proton image was acquired (FOV = 40 cm, matrix = 64×64×64, TE = 0.22 ms, TR = 2.1 ms, BW = 62.5 kHz, flip-angle = 5°, 5647 radial projections).

Image Processing and Analysis

In 9 of the 13 subjects undesirable signal from gas contamination was removed from the dissolved-phase signal in the HP [129]Xe data as previously described [20]. For all subjects, gas- and dissolved-phase k-space data were interpolated onto a Cartesian grid [21] using sampling density compensation weights estimated iteratively [22] to account for the non-uniformly sampled k-space coordinates. Images were then generated by inverse Fourier transform of the resulting resampled k-space data.

RBC and barrier components were separated using a whole lung RBC:Barrier ratio measured from a separate calibration scan [8]. Using the phase separation measured from the calibration scan, complex-valued dissolved-phase images were rotated by an increasing phase until the whole lung ratio of the real-to-imaginary image components matched the measured whole lung RBC:Barrier ratio for each subject. Following this rotation, the images of the RBC and barrier compartments were extracted from the real and imaginary components, respectively. These raw RBC and barrier component images were then converted to absolute RBC:Gas, Barrier:Gas and RBC:Barrier ratio images for further analysis [23].

Parametric maps of the absolute RBC:Gas and Barrier:Gas ratios were binned into discrete histograms based on reference distributions generated from a heathy subject cohort reported previously [23]. These reference distributions were used to classify the human subject maps by color based on the number of standard deviations from the reference normal mean, and to generate discretized regional parametric maps for qualitative visual assessment.

Lung regions were then segmented semi-automatically from the registered proton MRI and used to define voxels for HP [129]Xe ventilation and dissolved phase analyses. Thoracic 3D proton images were registered to the HP [129]Xe ventilation images using an affine

transformation. Lung volumes were determined by multiplying the number of voxels within the registered lung masks by the voxel volume. Differences in lung inflation volume were calculated between visits for each subject.

Statistical Analysis

Quantitative analysis was performed both on the entire cohort, and on only the subset of subjects where gas contamination correction was possible. Notably, this correction could be applied to all subjects for which PFT data was available.

The mean and standard deviations of Barrier:Gas, RBC:Gas and RBC:Barrier ratio distributions were compared across time points using Bland Altman plots [24] and further quantified using the intra-class correlation coefficient (ICC) [25], coefficient of repeatability (CR) and coefficient of variation (CV), the latter of which is simply the standard deviation expressed as a percentage of the mean, while the CR is the 95% confidence limit of expected absolute inter-measurement differences. Similar analysis was performed to determine the repeatability of FEV1 %p, FVC %p and DL_{CO} %p for a total of 9 measures (6 image measures and 3 PFT measures). Computed ICCs were considered significantly greater than 0 when $P < 0.05$ (using an F-test).

The influence of lung volume on the ^{129}Xe gas-exchange ratios was investigated by computing Pearson correlation coefficients between the relative changes in lung inflation volume between subject visits and the relative changes in Barrier:Gas, RBC:Gas and RBC:Barrier ratios. Where correlations were significant ($P < 0.05$), a linear regression model was fit, and deviations from a one-to-one relationship were tested by computing p-values for the null hypothesis that the constant and linear coefficients of the models were equal to 0 and unity, respectively. The linear fit was then used to correct the Barrier:Gas and RBC:Gas ratios at the 2nd visit by accounting for (i.e. subtracting out) the predicted differences associated with the known changes in lung volume. The CV of the corrected ratios was then compared to the uncorrected measurements.

Finally, Spearman correlations were computed between whole-lung mean ^{129}Xe gas-exchange ratios and %p FEV1, FVC and DL_{CO}. Correlations between relative visit-to-visit differences in these same measures were also explored. All correlations were considered statistically significant when $P < 0.05$.

RESULTS

Technical success was achieved for both visits in 13 of 14 subjects recruited. One subject was unable to complete the imaging study due to low oxygen saturation during imaging. The volume of gas in the HP ^{129}Xe dose delivered was 0.96L ± 0.03L for the entire study population, with a difference of -0.01L ± 0.026L between study visits. Polarization of the dose of gas delivered was 18.4% ± 3.9% for the entire study population, with a difference of 1.3% ± 3.8% across study visits.

Bland Altman plots of the mean and standard deviations of the distributions of each of the three ^{129}Xe dissolved-phase measures of interest are shown in Figure 1. No measure

demonstrated statistically significant bias between visits. The whole lung mean of the Barrier:Gas (Figure 1a) and RBC:Gas (Figure 1b) distributions for each subject were less reproducible than the mean RBC:Barrier (Figure 1c), with CVs of 19.2%, 20.0% and 11.5%, respectively. Notably, these CVs all decreased after excluding the 3 subjects without correction for gas contamination [20], and RBC:Barrier remains more reproducible than the other ratios (CVs reduced to 15.8%, 16.5% and 6.2%, respectively). The standard deviations of these metrics (Figures 1d-f) all have similar CVs (18.5%–25%).. Measures of FEV1 and FVC (Table 2) were in general extremely reproducible (CV <= 3.1%), which is in line with previous estimates in healthy subjects [25]. However, DL_{CO} was less repeatable (CV = 12.5%), and much less so than in previously reported [26]. Notably, a single subject appears to contribute much of the variability in DL_{CO} (%p DL_{CO} of 69% and 95% at visits 1 and 2, CV = 22.4%), supported by the fact that removing that subject reduces the CV to 6.3%, which is in closer agreement with the previous literature [27]. Also of note, the ICC was statistically significant for all measures. A full summary of the variability and ICC for these measurements is provided in Table 2.

The correlations between mean ^{129}Xe MRI dissolved-phase measures and pulmonary function tests are summarized in Table 3. Strong correlations were singularly found between the RBC:Barrier and FEV1 (r=0.75, *P*=0.002). Interestingly, for a given visit time point none of the dissolved phase measures were significantly correlated with DL_{CO} in this healthy cohort, although correlations between RBC:Barrier and DL_{CO} were nearly so. However, the respective change in inter-visit RBC:Barrier for each subject was significantly correlated with corresponding change in DL_{CO} (r=0.93, *P*=0.007). No other relationships were found for change in either Barrier:Gas or RBC:Gas and any PFT measures. No significant correlations were found between changes in PFT measures with each other, including FEV1, FVC and DLCO over the two-visits.

For dependencies on lung inflation volume, the change in relative lung volume across visits was found to be significantly correlated with change in both Barrier:Gas (r=−0.73, *P*=0.005) and RBC:Gas (r=−0.69, *P*=0.009), but not RBC:Barrier (r=−0.24, *P*=0.44). Scatterplots of these relationships are shown in Figure 2, along with a plot of the linear regression fit to each pair of measurements. For the significant correlations, tests of the null hypotheses that the intercepts (β_0) of these fits are different from 0 cannot be rejected (Barrier:Gas - β_0 = −0.41, *P*=0.91; RBC:Gas - β_0 = 4.76, *P*=0.36), and tests of the null hypothesis that the slopes (β_1) are equal to −1 cannot be rejected (Barrier:Gas - β_1 = −1.00, *P*=0.97; RBC:Gas - β_1 = −0.96, *P*=0.87), supporting a strong one-to-one relationship between relative changes in lung volume and relative changes in both Barrier:Gas and RBC:Gas measurements. Excluding the 3 subjects without correction for gas contamination did not significantly change these results. We found the CV in the Barrier:Gas and RBC:Gas measurements is reduced from 19.2% and 20.0% to 10.9% and 12.6%, respectively, after lung volume adjustment using the estimated linear models to remove visit-to-visit variations. Notably, these CVs are comparable to the RBC:Barrier CV (11.5%).

Histograms of the Barrier:Gas, RBC:Gas and RBC:Barrier distributions in all 13 subjects are shown in Figure S1. Qualitatively the inter-visit agreement for each signal bin is good in the majority of cases for all three ratio measures, although there are individual exceptions. This

supports the quantitative evaluation of the mean and standard deviation of these distributions already shown. This visual assessment indicates that the shapes of the distributions across visits seem to match qualitatively quite well. It also appears that there is greater inter-subject than inter-visit variation in the shape of the distributions, even in this healthy subject cohort.

Regional inter-visit comparisons were explored qualitatively by comparing parametric maps of the three ^{129}Xe dissolved-phase measures across visits in a subset of subjects, shown in Figures 3, 4, and 5. These specific subjects represent a range of cases where visit-to-visit lung volume increased, decreased and stayed relatively consistent. Subject A (top row) had a ~14% decrease in lung volume at visit 2, consistent with a downward shift in the Barrier:Gas and RBC:Gas distributions. Subject B (middle row) had a ~4% increase in lung volume at visit 2, again in agreement with a nearly equivalent, yet slightly higher, mean in the Barrier:Gas and RBC:Gas distributions at the 2nd time point. Finally, subject C (bottom row) had a large, ~18% decrease in lung volume at the 2nd visit, associated with greatly increased Barrier:Gas and RBC:Gas measures. The impact of the differences in lung inflation volume on the RBC:Barrier distributions is much less apparent, again consistent with the previous analysis of the whole lung mean values. Importantly, the spatial patterns of all three of these metrics, i.e. regions of *relatively* low and high intensity, appear to match quite well across visits regardless of lung volume differences. Overall it seems apparent that there is more variation in the regional patterns of ^{129}Xe dissolved-phase measures between subjects than between visits.

DISCUSSION

We present a rigorous quantitative study of the repeatability of the regional of hyperpolarized ^{129}Xe dissolved phase Barrier:Gas, RBC:Gas and RBC:Barrier ratios of gas-exchange derived from 3D radial spectroscopic imaging. The results indicate high repeatability of the whole lung mean values, especially for RBC:Barrier. The values we report are generally in agreement with previous estimates measured with whole lung spectroscopy [12] and alternative regional spectroscopic imaging methods [16]. It is possible to begin to estimate coefficients of repeatability (CR) for dissolved phase ratios necessary to evaluate progression. Based on our Bland-Altman analysis, these CR's are 0.37, 0.14, and 0.09 for whole lung mean values of the Barrier:Gas, RBC:Gas and RBC:Barrier ratios, respectively. In our study the RBC:Barrier ratio was not dependent on lung inflation volume, while both Barrier:Gas and RBC:Gas were moderate-to-strongly dependent on lung inflation volume. These results suggest RBC:Barrier ratio is a candidate image biomarker of progression for chronic lung diseases impacting gas exchange.

The standard deviations across the lung were also repeatable, but more variable due to expected variations in SNR and regional physiology. Indeed, the standard deviation of the RBC:Barrier ratio is negatively correlated with gas polarization (r=−0.54, P=0.008). It is important to consider visit-to-visit changes in the underlying pulmonary function or physiology that could also influence the expected repeatability. No indication of any such events was indicated by pulmonary function tests, specifically FEV1 and FVC, which were extremely repeatable with CR = ±4.6 %p and CR = ±6.1 %p over the two visits, respectively. DL_{CO} and RBC:Barrier have been shown to be highly correlated in disease

populations [12,14], and the CV for these two measurements were, in fact, comparable. Interestingly, the change in inter-visit RBC:Barrier were *strongly* correlated with corresponding change in DL_{CO}, which points to longitudinal intra-subject changes in RBC:Barrier as a potential regional biomarker for monitoring individual progression or response to interventions [14].

Correlations between Barrier:Gas and RBC:Gas metrics and pulmonary function tests were generally low, which was somewhat surprising given strong associations reported in prior studies. Previous work has shown moderate-to-strong correlations between all these [129]Xe gas-exchange metrics (measured with whole lung spectroscopy) and both FVC and DL_{CO} [9]. A few potential explanations include the following. First, the previously mentioned work had a cohort including both healthy volunteers and patients with idiopathic pulmonary fibrosis (IPF) diagnoses, and correlations were not reported for these groups separately. It is possible that controlling for disease state would account for a significant portion of these correlations, given that the population means of FVC, DL_{CO} and [129]Xe gas-exchange metrics in healthy and IPF patients were all shown to be significantly different [9]. Second, only 7 subjects in our cohort had all PFT measurements acquired at both time points, limiting statistical power. Third, our longitudinal comparisons showed that lung volume variations add significant variance to both Barrier:Gas and RBC:Gas estimates, representing an additional source of noise. Some combination of these explanations seems most likely.

The moderate-to-strong dependence of Barrier:Gas and RBC:Gas on lung volume is generally in agreement with previous work using whole lung spectroscopy, which reported a dependence of all three [129]Xe gas-exchange ratios on lung inflation level [15]. While we did not detect a relationship between lung volume and RBC:Barrier, it should be noted that the Qing et al. [15] work demonstrated a much smaller dependence for RBC:Barrier than that found in either Barrier:Gas or RBC:Gas. Moreover, the Qing et al. work probed a much larger range of lung volumes (ranging from RV to TLC) and differences in RBC:Barrier only reached significance for comparisons between RV and TLC. Such an extreme change in lung inflation volume could lead to differences in alveolar pressure (and thus capillary blood volume) associated with breath hold. Such differences in capillary blood volumes are less likely to vary significantly in the range of ±15% around FRC + 1L that is explored in the current work.

There are a few limitations that are important to consider. As mentioned, the subject cohort is relatively small, especially the proportion for which PFT measurements are available and complete, limiting the statistical power given the small number of comparisons available. Second, the data was acquired using a single imaging technique (1-point Dixon) and a single set of sequence parameters (e.g. flip angles, TR, image resolution, etc.), and may be specific to this methodology. It cannot be assumed that this repeatability is representative of other methodologies for measuring [129]Xe gas-exchange measures (e.g. IDEAL based techniques) [6], and may also vary with different acquisition parameters [28]. Refinements to protocol selection and acceptance of a common methodology and approach are necessary to optimally position [129]Xe gas-exchange MRI for clinical application. Third, a subset of the patients was imaged without utilizing a multi-echo sequence, which prevents the removal of any potential gas phase contamination of the dissolved phase data [20]. It is likely the

general increase in variability (particularly in mean dissolved phase measures) when including these cases is due to residual gas contamination, and is likely the cause for the large (−50%) inter-visit RBC/barrier change seen in one subject (see Figure 2). Fourth, the data presented are in healthy subjects who may tolerate the exam better than diseased subjects. Repeatability may differ for subjects with disease, especially given that illness may impact breath-hold duration and introduce additional uncertainties due to motion or partial inhalation of the gas dose. Finally, regional parametric maps were analyzed qualitatively, and future work incorporating more regionalized quantitative analyses could potentially be performed by utilizing spatial registration and voxel-wise comparisions or using metrics of spatial heterogeneity [29].

In conclusion, we have presented data characterizing the repeatability of regional ^{129}Xe gas-exchange metrics estimated using a 1-point Dixon technique. The work shows excellent repeatability for three commonly used measures and especially Barrier:RBC ratio. In addition, controlling for lung volume is shown to be similarly important for regional measures as it is for global spectroscopy to avoid systematic bias, especially for Barrier:Gas and RBC:Gas ratios. More qualitatively, regional patterns in these measurements appear robust. These results inform future study designs and minimum thresholds for monitoring disease progression.

Supplementary Material

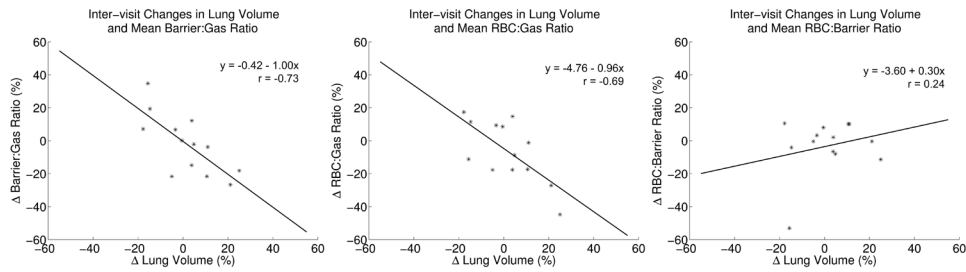Refer to Web version on PubMed Central for supplementary material.

REFERENCES

1. Ebner L, Kammerman J, Driehuys B, Schiebler ML, Cadman RV, Fain SB. The role of hyperpolarized 129Xenon in MR imaging of pulmonary function. Eur J Radiol 2017; 86:343–352. [PubMed: 27707585]

2. Kirby M, Svenningsen S, Owrangi A, Wheatley A, Farag A, Ouriadov A, Santyr GE, Etemad-Rezai R, Coxson HO, McCormack DG, Parraga G. Hyperpolarized 3He and 129Xe MR imaging in healthy volunteers and patients with chronic obstructive pulmonary disease. Radiology 2012; 265(2):600–610. [PubMed: 22952383]

3. Chen RY, Fan FC, Kim S, Jan KM, Usami S, Chien S. Tissue-blood partition coefficient for xenon: temperature and hematocrit dependence. J Appl Physiol 1980; 49(2):178–183. [PubMed: 7400000]

4. Cleveland ZE, Cofer GP, Metz G, et al. Hyperpolarized 129Xe MR imaging of alveolar gas uptake in humans. PLos ONE 2010:5:e12192. [PubMed: 20808950]

5. Mugler JP III, Altes TA, Ruset IC, Dregely IM, Mata JF, Miller GW, Ketel S, Ketel J, Hersman FW, Ruppert K. Simultaneous magnetic resonance imaging of ventilation distribution and gas uptake in the human lung using hyperpolarized xenon-129. Proc Natl Acad Sci 2010; 107:21707–21712. [PubMed: 21098267]

6. Qing K, Ruppert K, Jiang Y, et al. Regional mapping of gas uptake by blood and tissue in the human lung using hyperpolarized xenon-129 MRI. J Magn Reson Imaging 2014; 39:346–359. [PubMed: 23681559]

7. Patz S, Muradyan I, Hrovat M, Dabaghyan M, Washko G, Hatabu H, Butler JP. Diffusion of hyperpolarized 129 Xe in the lung: a simplified model of 129 Xe septal uptake and experimental results. New J Phys 2011; 13:015009.

8. Kaushik SS, Robertson SH, Freeman MS, He M, Kelly KT, Roos JE, Rackley CR, Foster WM, McAdams HP, Driehuys B. Single-Breath Clinical Imaging of Hyperpolarized ^{129}Xe in the Airspaces, Barrier and Red Blood Cells using an Interleaved 3D Radial 1-point Dixon Acquisition. Magn Reson Med. 2016; 75(4):1434–1443. [PubMed: 25980630]

9. Wang JM, Robertson SH, Wang Z, He M, Virgincar RS, Schrank GM, Smigla RM, O'Riordan TG, Sundy J, Ebner L, Racley CR, McAdams HP, Driehuys B. Using Hyperpolarized 129Xe to Quantify Regional Gas Transfer in Idiopathic Pulmonary Fibrosis. Thorax 2018; 73(1):21–28. [PubMed: 28860333]

10. Galbraith SM, Lodge MA, Taylor NJ, Rustin GJS, Bentzen S, Stirling JJ, Padhani AR. Reproducibility of dynamic contrast-enhanced MRI in human muscle and tumours: comparison of quantitative and semiquantitative analysis. NMR Biomed 2002;15:132–142. [PubMed: 11870909]

11. Stewart NJ, Leung G, Norquay G, et al. Experimental validation of the hyperpolarized 129Xe chemical shift saturation recovery technique in healthy volunteers and subjects with interstitial lung disease. Magn Reson Med 2015; 74:196–207. [PubMed: 25106025]

12. Stewart NJ, Horn FC, Norquay G, Collier GJ, Yates DP, Lawson R, Marshall H, Wild JM. Reproducibility of Quantitative Indices of Lung Function and Microstructure from 129Xe Chemical Shift Saturation Recovery (CSSR) MR Spectroscopy. Magn Reson Med 2017; 77:2107–2113. [PubMed: 27366901]

13. Kaushik SS, Freeman MS, Yoon SW, Liljeroth MG, Stiles JV, Roos JE, Foster WM, Rackley CR, McAdams HP, Driehuys B. Measuring Diffusion-Limitation with a Perfusion-Limited Gas-Hyperpolarized ^{129}Xe Gas-Transfer Spectroscopy in Patients with Idiopathic Pulmonary Fibrosis. J Appl Physiol. 2014; 117:577–585. [PubMed: 25038105]

14. Weatherley ND, Stewart NJ, Chan HF, Austin M, Smith LJ, Collier G, Rao M, Marshall H, Norquay G, Renshaw SA, Bianchi SM, Wild JM. Hyperpolarised xenon magnetic resonance spectroscopy for the longitudinal assessment of changes in gas diffusion in IPF. Thorax 2018. pii: thoraxjnl-2018–211851. doi: 10.1136/thoraxjnl-2018-211851. [Epub ahead of print]

15. Qing K, Mugler JP, Altes TA, Jiang Y, Mata JF, Miller GW, Ruset IC, Hersman FW, Ruppert K. Assessment of Lung Function in Asthma and COPD using Hyperpolarized 129Xe Chemical Shift Saturation Recovery Spectroscopy and Dissolved-Phase MR Imaging. NMR Biomed 2014; 27(12):1490–1501. [PubMed: 25146558]

16. Kern AL, Gutberlet M, Qing K, Voskrebenzev A, Klimes F, Kaireit TF, Czerner CP, Biller H, Wacker F, Ruppert K, Hohlfeld JM, Vogel-Claussen J. Regional Investigation of Lung Function and Microstructure Parameters by Localized ^{129}Xe Chemical Shift Saturation Recovery and Dissolved-phase Imaging: A Reproducibility Study. Magn Reson Med. 2019;81:13–24. [PubMed: 30198113]

17. Lynch DA, Sverzellati N, Travis WD, Brown KK, Colby TV, Galvin JR, et al. Diagnostic criteria for idiopathic pulmonary fibrosis: a Fleischner Society White Paper. Lancet Respir Med. 2018;6(2):138–53. [PubMed: 29154106]

18. Quanjer PH, Stanojevic S, Cole TJ, Baur X, Hall GL, Culver BH, Enright PL, Hankinson JL, Ip MS, Zheng J, Stocks J, ERS Global Lung Function Initiative. Multi-ethnic reference values for spirometry for the 3–95-yr age range: the global lung function 2012 equations. Eur Respir J. 2012; 40(6):1324–43. [PubMed: 22743675]

19. Driehuys B, Cates GD, Miron E, Sauer K, Walter DK, Happer W. High-volume production of laser-polarized Xe-129. Apply Phys Lett. 1996; 69:1668–1670.

20. Hahn AD, Kammerman J, Fain SB. Removal of Hyperpolarized ^{129}Xe Gas-phase Contamination in Spectroscopic Imaging of the Lungs. Magn Reson Med 2018:doi:10.1002/mrm.27349.

21. Jackson J, Meyer CH, Nishimura DG, Macovski A. Selection of a convolution function for Fourier inversion using gridding. IEEE Trans Med Imaging. 1991; 10:473–478. [PubMed: 18222850]

22. Pipe JG, Menon P. Sampling density compensation in MRI: rationale and an iterative numerical solution. Magn Reson Med. 1999; 41:179–186. [PubMed: 10025627]

23. Wang Z, Robertson SH, Wang J, He M, Virgincar RS, Schrank GM, Bier EA, Rajagopal S, Huang YC, O'Riordan TG, Rackley CR, McAdams HP, Driehuys B. Quantitative analysis of hyperpolarized 129Xe gas transfer MRI. Med Phys. 2017; 44(6):2415–2428. [PubMed: 28382694]

24. Bland JM, Altman DG. Measuring agreement in method comparison studies. Stat Methods Med Res 1999; 8:135–160. [PubMed: 10501650]

25. Bartko JJ. The Intraclass Correlation Coefficient as a Measure of Reliability. Psychological Reports 1966; 19(1): 3–11. [PubMed: 5942109]

26. Enright PL, Johnson LR, Connett JE, Voelker H, Buist AS. Spirometry in the Lung of Health Study. 1. Methods of Quality and Control. Am Rev Respir Dis. 1991; 143(6):1215–1223. [PubMed: 2048803]

27. Punjabi NM, Shade D, Patel AM, Wise RA. Measurement Variability in Single-Breath Diffusing Capacity of the Lung. Chest. 2003; 123(4):1082–1089. [PubMed: 12684297]

28. Ruppert K, Amzajerdian F, Hamedani H, Xin Y, Loza L, Achekzai T, Duncan IF, Profka H, Siddigui S, Pourfathi M, Sertic F, Cereda MF, Kadlecek S, Rizi RR. Assessment of flip angle-TR Equivalence for standardized dissolved-phase imaging of the lung with hyperpolarized 129Xe MRI. Magn Reson Med. 2018:doi:10.1002/mrm.27538.

29. Tzeng YS, Lutchen K, Albert M. The difference in ventilation heterogeneity between asthmatic and healthy subjects quantified using hyperpolarized 3He MRI. J Appl Physiol 2009; 106(3):813–22. [PubMed: 19023025]
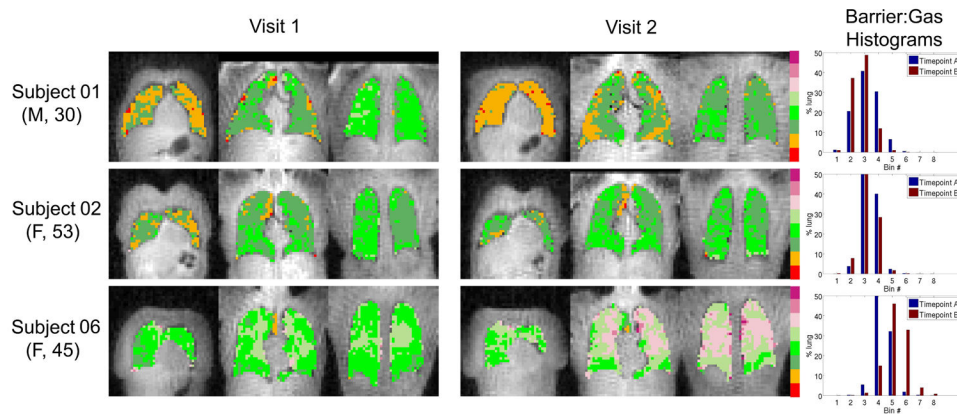
Figure 1.

Bland Altman plots indicating repeatability of Barrier:Gas mean (a), RBC:Gas mean (b), RBC:Barrier mean (c), Barrier:Gas standard deviation (d), RBC:Gas standard deviation (e) and RBC:Barrier standard deviation (f). Solid and dotted lines show the mean and 95% confidence intervals, respectively, of inter-visit differences. Coefficients of repeatability (CR) and coefficients of variation (CV) are also indicated for each metric.
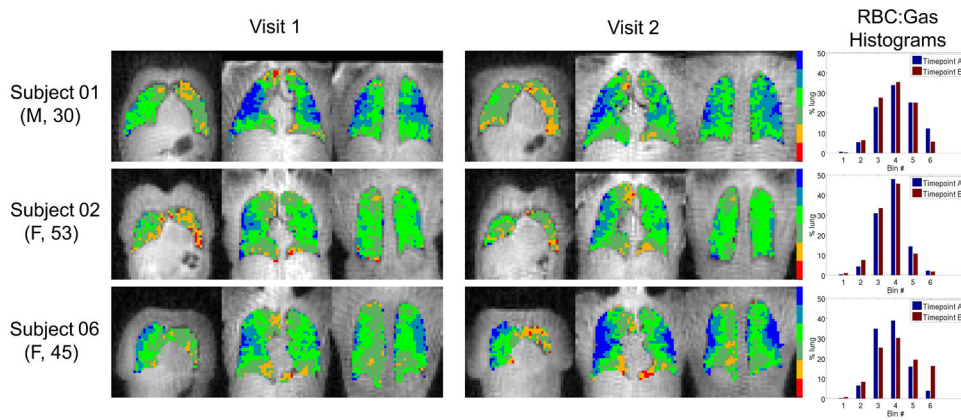
Figure 2.
Scatterplots of the relative inter-visit differences vs lung volume and mean Barrier:Gas (a), RBC:Gas (b) and RBC:Barrier (c). Lines show the fit of a linear regression in each plot, with the equation of the line along with correlation coefficients provided as well. Significant correlations between changes in lung volume and both Barrier:Gas and RBC:Gas were found, and these relationships were roughly equivalent.
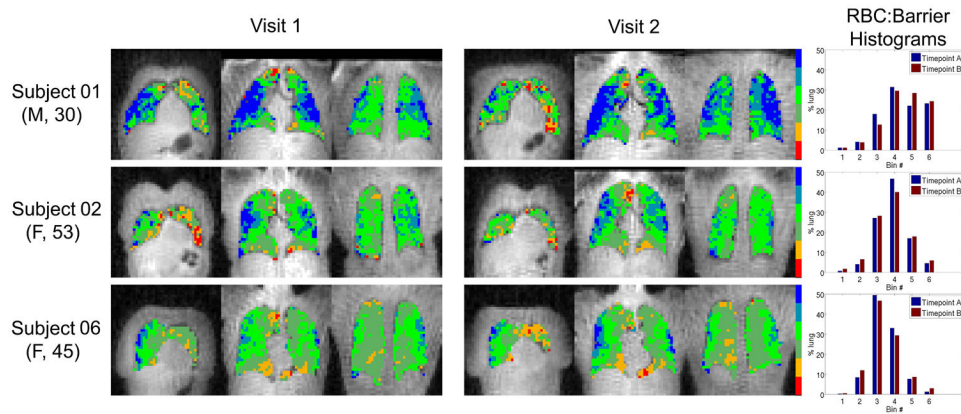
Figure 3.

Parametric maps of Barrier:Gas (binned according to a reference distribution mean and standard deviation) in coronal slices from 3 different subjects at both visits. Lung volumes were approximately +14%, +4% and −18% different at visit 2 for subjects 01, 02 and 06, respectively. Smaller visit 2 lung volumes (e.g. Subject 06) were associated with higher visit 2 Barrier:Gas, and vice versa (e.g. Subject 01). Spatial distributions of regions of relatively high and low Barrier:Gas appear relatively well matched between visits. Subject numbers correspond to those in Table 1. Numerical cutoff values between Barrier:Gas bins (from smallest to largest) were [0.26, 0.64, 1.03, 1.42, 1.81, 2.20, 2.58].

Figure 4.
Parametric maps of RBC:Gas (binned according to a reference distribution mean and standard deviation) in coronal slices from 3 different subjects at both visits (subjects and slices shown are identical to those presented in Figure 4). Lung volumes were approximately +14%, +4% and −18% different at visit 2 for subjects 01, 02 and 06, respectively. Smaller visit 2 lung volumes (e.g. Subject 06) were associated with higher visit 2 RBC:Gas, and vice versa (e.g. Subject 01). Spatial distributions of regions of relatively high and low RBC:Gas appear relatively well matched between visits. Subject numbers correspond to those in Table 1. Numerical cutoff values between RBC:Gas bins (from smallest to largest) were [−0.19, 0.07, 0.33, 0.60, 0.86].

Figure 5.

Parametric maps of RBC:Barrier (binned according to a reference distribution mean and standard deviation) in coronal slices from 3 different subjects at both visits (subjects and slices shown are identical to those presented in Figures 4 and 5). Lung volumes were approximately +14%, +4% and −18% different at visit 2 for subjects 01, 02 and 06, respectively. Lung volume differences did not appear to have a significant influence on the RBC:Barrier ratio, and spatial distributions of regions of relatively high and low RBC:Barrier appear relatively well matched between visits. Subject numbers correspond to those in Table 1. Numerical cutoff values between RBC:Barrier bins (from smallest to largest) were [−0.17, 0.07, 0.32, 0.56, 0.80].

Table 1.

Subject Cohort Demographics and PFTs

Subject ID	Sex	Age	FEV1$_{\%p}$	FVC$_{\%p}$	DLCO$_{\%p}$
01	M	30	---	---	---
02	F	53	109%	107%	74%
03	M	59	---	---	---
04	F	56	90%	96%	69%
05	M	63	---	---	---
06	F	45	90%	88%	105%
07	M	68	104%	95%	105%
08	M	69	83%	86%	69%
09	F	65	99%	113%	97%
10	F	24	---	---	---
11	F	50	---	---	---
12	F	64	---	---	---
13	F	54	105%	113%	107%
Popluation	5M/8F	53.8 ± 13.9 yrs	97.1% ± 9.6%	99.7% ± 11.3%	89.4% ± 17.9%

Subject cohort sexes and mean ± standard deviation age and PFTs at baseline visit 1.

Table 2.

Repeatability of ^{129}Xe Gas-Exchange Metrics and Pulmonary Function Tests

Metric	Coefficient of Repeatability (CR)	Coefficient of Variation (CV)	Intra-class Correlation Coefficient (ICC)	ICC *P*-value
Mean Barrier:Gas	0.37	19.2%	0.78	<0.001
Mean RBC:Gas	0.14	20.0%	0.79	<0.001
Mean RBC:Barrier	0.09	11.5%	0.92	<0.001
Std. Dev. Barrier:Gas	0.11	19.6%	0.65	0.004
Std. Dev. RBC:Gas	0.10	18.5%	0.81	<0.001
Std. Dev. RBC:Barrier	0.19	25.0%	0.78	<0.001
$FEV1_{\%p}$	4.6	2.4%	0.97	<0.001
$FVC_{\%p}$	6.1	3.1%	0.96	<0.001
$DL_{CO,\%p}$	22.2	12.5%	0.79	0.006

Coeffiecients of variance and intra-class correlations for inter-visit comparisons of ^{129}Xe dissolved phase measures and PFTs.

Table 3.

Correlations Between Mean ^{129}Xe Gas-Exchange Metrics and Pulmonary Function Tests

	FEV1$_{\%p}$	FVC$_{\%p}$	DL$_{CO,\%p}$	FEV1$_{\%p}$	FVC$_{\%p}$	DL$_{CO,\%p}$
Barrier:Gas	−0.30 (0.29)	−0.39 (0.18)	0.09 (0.76)	-	-	-
RBC:Gas	0.39 (0.17)	−0.10 (0.73)	0.45 (0.10)	-	-	-
RBC:Barrier	**0.75** (0.002)	0.42 (0.14)	0.553 (0.05)	-	-	-
Barrier:Gas	-	-	-	−0.68 (0.11)	−0.36 (0.44)	0.18 (0.71)
RBC:Gas	-	-	-	−0.57 (0.20)	−0.14 (0.78)	0.39 (0.40)
RBC:Barrier	-	-	-	−0.14 (0.78)	0.32 (0.49)	**0.93** (0.007)

Spearman correlations between mean absolute ^{129}Xe gas-exchange metrics and pulmonary function tests, as well as correlations between the inter-visit, intra-subject differences in identical measures. *P*-values are indicated for each correlation in parentheses and significant correlations are shown with bold text.